NJC

Accepted Manuscript

This article can be cited before page numbers have been issued, to do this please use: M. R. Nabid, Y. Bide and B. Etemadi, *New J. Chem.*, 2017, DOI: 10.1039/C7NJ01108C.

ROYAL SOCIETY OF CHEMISTRY

rsc.li/njc

View Article Online
DOI: 10.1039/C7NJ01108C

Ag@Pd nanoparticles immobilized on nitrogen doped graphene carbon nanotube aerogel as a superb catalyst for dehydrogenation of formic acid

Mohammad Reza Nabid*, Yasamin Bide, Bahare Etemadi

Department of Polymer & Material Chemistry, Faculty of Chemistry & Petroleum Science, Shahid Beheshti University, G.C., P.O. Box 1983969411 Tehran, Iran.

Abstract

Nitrogen doped graphene carbon nanotube aerogel was successfully synthesized through a hydrothermal reaction and employed as an excellent support for immobilizing silver core palladium shell nanoparticles. The catalytic activity of the as obtained material was examined for dehydrogenation of formic acid as one of the most important catalytic reactions due to the critical global need for green energy and great features of formic acid as a hydrogen carrier. The effect of the support as well as the metal composition in the catalyst structure were studied for formic acid decomposition. The turnover frequency (TOF) over Ag@Pd/N-GCNT aerogel was measured to be 413 h^{-1} at 298 K which showed the superior activity of the presented catalyst for formic acid dehydrogenation without any additives. The activation energy of the reaction was calculated by the Arrhenius plot of ln TOF versus 1/T for the catalyst to be 29.28 kJ/mol which is lower than most of the reported values. In addition, the recyclability tests exhibit no significant change in catalytic efficiency after four runs.

* Corresponding author: Fax: +98 21 22431661. Tel: +98 21 29903102.
E-mail address: m-nabid@sbu.ac.ir (M. R. Nabid).

View Article Online
DOI: 10.1039/C7NJ01108C

Keywords: Graphene carbon nanotube aerogel; Doping; Core-shell; Catalysis; Dehydrogenation; Formic acid.

1. Introduction

Hydrogen (H_2) is expected to play an important role in future renewable energy technologies although effective hydrogen storage technologies still need to be developed.[1-3] The high density of hydrogen storage and direct conversion to electrical energy in fuel cells are some advantages of chemical storage over physical storage.[4] The usage of bio-renewable formic acid (FA) as a hydrogen carrier is attracting more and more attention owing to the several important features including renewable chemical synthesis, nontoxicity, high stability as a liquid at room temperature, high hydrogen content (4.4 wt%) and sustainable energy production.[5, 6] But, in the absence of suitable catalyst, the selectivity for FA decomposition to CO_2 and H_2 is poor due to the formation of H_2O and CO. Although the first reaction is thermodynamically favored but the energy barrier is high. So far, a large number of both heterogeneous and homogeneous catalysts have been studied for FA dehydrogenation.[7-10] Heterogeneous catalysts have attracted so much attention due to their advantages of operating at lower temperatures as well as facile catalyst separation and recycling.[11, 12] Among different heterogeneous catalyst systems, metal nanoparticle (MNP) catalysts have been extensively investigated but usually suffer from severe aggregation and limited catalytic activities.[13, 14] Among various active metals, Pd,[15, 16] Pt[17] and Au[18, 19] based catalysts are main catalytic metals. But, using Pt without surface modification or alloying cause to severe CO poisoning[17] and for Au, subnanometric clusters are necessary to give high catalytic activity[20] which limits their scale up application. More significantly, compared to Pt and Au, Pd is cheaper. So, Pd based catalysts are most attractive metal based systems for hydrogen generation from FA.[21-,23] It was found that bimetallic

View Article Online
DOI: 10.1039/C7NJ01108C

nanoparticles enhanced the activity and selectivity compared to their single component counterparts for the dehydrogenation of FA.[24] To increase the CO resistance and catalytic performance, Ag was chosen as the secondary metal to modify Pd, owing to more significant electronic promotion effect than other noble metals because of the largest difference in work function between Pd (5.6 eV) and Ag (4.7 eV) as well as the charge transfer from Ag to Pd.[25] The support plays a critical role on the metal particles size and dispersion and consequently their catalytic activity.[26] In 2016, Bi et al. reported the synthesis of carbon-supported Pd nanoparticles as an effective way to boost efficiency for dehydrogenation of FA due to prominent surface electronic modulation.[27] In this work, nitrogen-doped graphene carbon nanotube (N-GCNT) aerogel was chosen as the support to immobilize Ag@Pd core shell nanoparticles. Graphene and carbon nanotube (CNT) have attracted much attention due to their high surface areas, enhanced mobility of charge carriers, and high stability.[28, 29] Moreover, CNT bridges the defects for electron transfer and inhibit the restacking of graphene sheets while graphene can simultaneously inhibit the aggregation of CNT.[30] The integration of graphene and CNT into a hybrid aerogel may enhance their dispersion and collect the fascinating properties of both materials as well as the unique characteristics of aerogels. Furthermore, nitrogen doping can induce unique optical, electrical and especially catalytic properties to the support.[31]

2. Experimental

2.1. Materials

Graphite powder (325 mesh), potassium peroxodisulfate ($K_2S_2O_8$), di-phosphorus pentoxide (P_2O_5), dicyandiamide and palladium chloride ($PdCl_2$) were purchased from Merck Chem. MWCNTs (dia.= 110–170 nm, length = 5–9 micron) and Silver nitrate ($AgNO_3$) were prepared

View Article Online
DOI: 10.1039/C7NJ01108C

from Aldrich company. All other chemicals were purchased from Aldrich or Merck companies and used as received without any further purification.

2.2. Instruments and characterization

Transmission electron microscopy (TEM) was performed by LEO 912AB electron microscope. X-ray powder diffraction (XRD) data were collected on an XD-3A diffractometer using Cu Kα radiation. X-ray photoelectron spectroscopy (XPS) was performed using a VG multilab 2000 spectrometer (ThermoVG scientific) in an ultrahigh vacuum. Scanning electron microscope (SEM) was performed on a Zeiss Supra 55 VP SEM instrument. The specific surface area was calculated using the Brunauer–Emmett–Teller (BET) equation using a PHS-1020(PHSCHINA) device. Pore size distribution was determined by Barrett–Joyner–Halenda (BJH) method. The sample was degassed at 150 ^{o}C for 20 h before measurements. AA-680 Shimadzu (Kyoto, Japan) flame atomic absorption spectrometer (AAS) with a deuterium background corrector was used for determination of the metals.

2.3. Synthesis of nitrogen doped graphene carbon nanotube aerogel

Graphene oxide (GO) was prepared through a modified Hummers method.[32, 33] In a typical procedure, a certain amount of CNTs (75 mg) and 0.75 mg polyvinylpyrrolidone (PVP) were added into 30 mL ethanol and the resulting mixture was sonicated for 5 h to form a dispersion (2.5 mg/mL). GO and CNTs solution with mass ratio of 3:1 with total volume of 40 mL were mixed and stirred for 1 h to form a uniform GO-CNTs dispersion. After that, 1.85 g (0.6 mmol) dicyandiamide was added and this dispersion was transferred into a Teflon-lined stainless steel autoclave and heated at 120 ^{o}C for 12 h to prepare graphene-CNTs hybrid hydrogel. The resulted hydrogel was washed with high-purity milli-Q water for several times and freeze-dried (-80 ^{o}C pre-cooling) 48 h to obtain the N-GCNT aerogel.

View Article Online
DOI: 10.1039/C7NJ01108C

2.4. Synthesis of Ag@Pd nanoparticles immobilized on nitrogen doped graphene carbon nanotube aerogel (Ag@Pd/N-GCNT aerogel)

Typically, for the preparation of Ag@Pd 1:1 ratio, in a 100 mL round bottom flask, 0.025g (0.23 mmol) of $AgNO_3$ and 0.34 g of N-GCNT aerogel were dissolved in 30 mL of ethylene glycol under stirring. The solution was slowly heated (7 ^oC/min) to 120^oC under N_2 atmosphere for half an hour. A solution containing 0.06 g (0.23 mmol) of $PdCl_2$ and 30 mL of ethylene glycol were added to the above mixture. The resulting solution was heated (7^oC/min) to 90^oC for 2 h under N_2 atmosphere. The obtained $Ag_1@Pd_1$/N-GCNT aerogel was washed with acetone twice and dried under N_2 atmosphere. The preparations of $Ag_1@Pd_2$/N-GCNT aerogel, $Ag_2@Pd_1$/N-GCNT aerogel, Ag/N-GCNT aerogel, and Pd/N-GCNT aerogel catalysts were synthesized with the above procedure except that the molar ratios of Ag and Pd were 1:2, 2:1, 1:0 and 0:1, respectively. The contents of Ag and Pd in the as obtained material were determined by AAS as shown in Table 1.

Table 1. AAS results of Ag@Pd/N-GCNT aerogel catalysts.

Catalysts	**Ag (wt%)**	**Pd (wt%)**	**Initial Ag:Pd ratio**	**Final Ag:Pd ratio**
$Ag_1@Pd_2$/N-GCNT aerogel	7.21	13.69	1:2	1:1.90
$Ag_1@Pd_1$/N-GCNT aerogel	10.34	9.68	1:1	1:0.94
$Ag_2@Pd_1$/N-GCNT aerogel	14.05	6.98	2:1	2.01:1

2.5. Hydrogen generation from formic acid aqueous solution

An aqueous suspension containing the as-prepared catalyst was placed in a two-neck round-bottom flask, which was placed in a water bath under ambient atmosphere. A gas burette filled

View Article Online
DOI: 10.1039/C7NJ01108C

with water was connected to the reaction flask to measure the volume of released gas. Firstly, 3 mg catalyst and 2 mL distilled water were placed in the round bottomed flask. The reaction was started when 1.5 mL of 1 mmol/mL aqueous solution of FA was injected into the sealed flask. The volume of the evolved gas was monitored by recording the displacement of water in the gas burette.

3. Results and discussion

3. 1. Synthesis and recognition of the catalyst

Morphological structure of the resulting Ag@Pd/N-GCNT aerogel has been verified by SEM and TEM as shown in Figure 1. From SEM image, it is observed that CNTs can exist on graphene wall, between two graphene sheets or in the middle of graphene sheets. Therefore, several forms between CNTs and graphene sheets induce the surface roughness of the sheets and consequently a cross linked structure between layers. The SEM image shows the porosity of the structure which in accordance with BET results. In addition, the numerous nanoparticles are observed in SEM image, but for further investigation TEM was necessary. The TEM image indicates that hybrid aerogel is composed of thin graphene sheets and tortuous CNTs. The Ag@Pd NPs are well dispersed and immobilized on the N-GCNT aerogel with particle size of 3-12 nm. According to TEM image, the support can prevent the Ag@Pd NPs from aggregation, which will benefit their catalytic performance. Because of almost no difference in contrast between the Ag as core and Pd as shell elements (Ag and Pd are next to each other in the periodic table), direct imaging of the core–shell by high-resolution TEM was failed.

View Article Online
DOI: 10.1039/C7NJ01108C

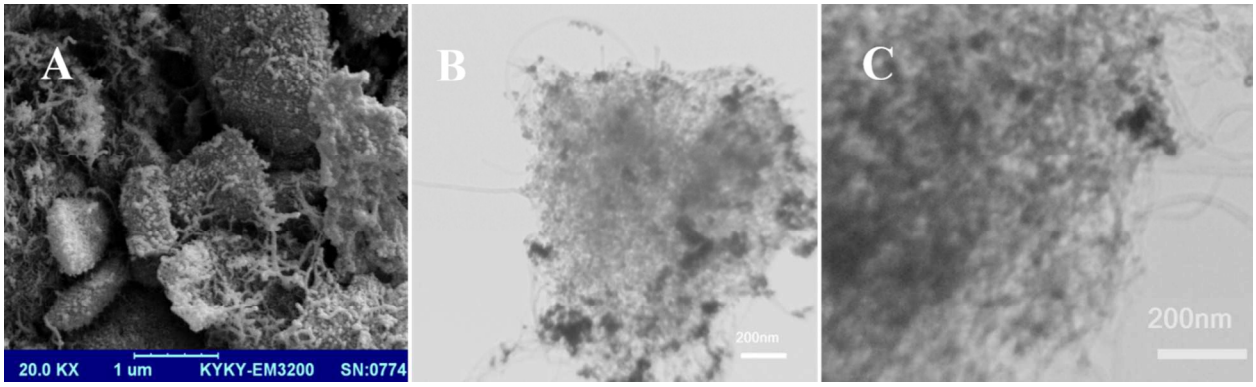

Fig. 1. SEM (A) and TEM (B and C) images of Ag@Pd/N-GCNT aerogel.

X-ray powder diffraction (XRD) has been used to determine the phase and structure of the synthesized materials as shown in Figure 2. The XRD pattern of CNT shows a broad peak at 25.88^{o} related to the (0 0 2) plane of the graphite like structure of the MWCNTs. In the XRD pattern of GO, the peak at 10.32^{o} is associated to the (0 0 2) plane of GO. In addition, a weak peak is observed at 2θ=20.3° indicating the existence of oxygen-based functional groups on the surface of the graphite.[34] After the synthesis of N-GCNT aerogel in the hydrothermal process, the diffraction peak at 25.48^{o} appeared demonstrating the development of graphitic structures. The XRD pattern of Ag@Pd nanoparticles immobilized on N-GCNT aerogel has been presented in Fig. 2. To clarify the structure of the catalyst, the XRD patterns of Ag@Pd, Ag and Pd nanoparticles immobilized on N-GCNT aerogel were provided (See ESI, Fig. S1). In the XRD pattern of Ag@Pd/N-GCNT aerogel, besides the peak of N-GCNT aerogel, a series of diffraction peaks at 39.73, 46.17, 64.37, 67.47, and 76.67° are existed. These peaks can be attributed to the combination of diffraction peaks of Pd/N-GCNT aerogel at 40.28, 46.82, and 68.18° corresponded to Pd (111), (200), and (220), respectively (Fig. S1) (JCPDS 04e0802) and Ag/N-GCNT aerogel at 38.29, 44.66, 64.66 and 77.71 assigned to Ag (111), (200), (220) and (311), respectively (Fig. S1) (JCPDS 04e0783) with a face-centered cubic structure.[35, 36] The XRD pattern shows a Pd-like pattern suggesting the Ag core Pd shell structure (Fig. S1).

View Article Online
DOI: 10.1039/C7NJ01108C

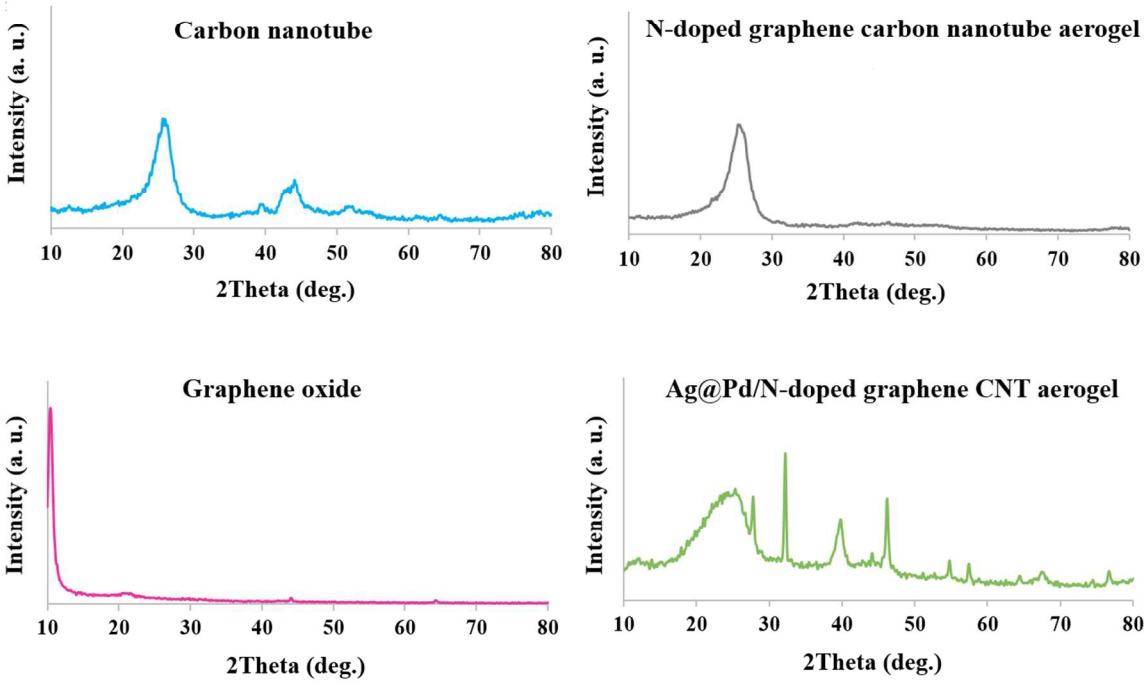

Fig. 2. XRD patterns of CNT, GO, N-GCNT aerogel, and Ag@Pd/N-GCNT aerogel.

In catalytic applications, the surface area is one of the most vital factors for a support. The N-GCNT aerogel displays a BET surface area of 381.8 m^2/g. The high porosity in the N-GCNT aerogel can be attributed to the fact that some CNTs bridges between graphene sheets preventing them from the restacking aggregation. Thus, the as obtained structure provides more voids and cavities available for N_2 adsorption. BET testing also showed a mesoporous structure (i.e., the pore size between 2 and 50 nm, defined by the IUPAC classification) with the average pore sizes of 15.4 nm from analysis of the adsorption branch by the Barrett–Joyner–Halenda (BJH) method. Because of the mesoporous structure of the aerogel, the BJH method was adopted to analyze the mesopore size distribution[37] (the inset of Figure 3).

View Article Online
DOI: 10.1039/C7NJ01108C

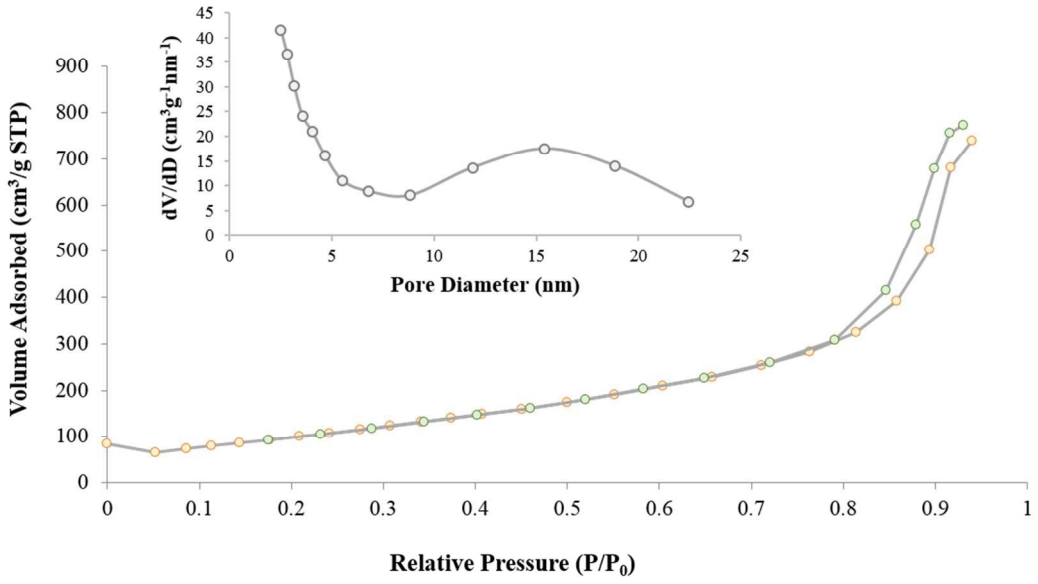

Fig. 3. Nitrogen adsorption isotherm of N-GCNT aerogel. The inset shows the pore-size distribution obtained from adsorption branch using the BJH method.

To investigate the electronic structure and composition of the as-prepared Ag@Pd/N-GCNT aerogel in detail, the XPS study was carried out. The XPS survey scan shows five elements, C, O, N, Ag and Pd, in the sample (Fig. 4A). The presence of nitrogen with the atom percentage of 2.8% confirms the successful doping of nitrogen into graphene carbon nanotube aerogel. The high resolution XPS C 1s spectrum (Fig. 4B) can be deconvoluted into four subpeaks, indicating the existence of four types of carbon. The peaks at 284.6, 285.3, 285.9 and 287.3 eV are assigned to graphite-like sp^2 C (C-C linkage), C-N, C-O and C=O linkages, respectively. The presence of the peak at 285.3 eV attributed to C−N confirms the substitution of the nitrogen atoms within graphene carbon nanotube aerogel. It is noteworthy that the lower intensity of C-O and C=O linkages peaks means the effective removal of oxygen containing groups after the hydrothermal process.[38] The high resolution peaks of N 1s, Pd 3d and Ag 3d are shown in Fig. S2. In the N 1s XPS core level spectrum, four peaks are observed at 397.7, 400.0, 401.2, and 403.6 eV attributed

View Article Online
DOI: 10.1039/C7NJ01108C

to the pyridinic N, pyrrolic N, quaternary N, and oxidized N, respectively.[39] XPS peaks of Pd $3d_{5/2}$ and Pd $3d_{3/2}$ are observable at 335.2 and 340.0 eV, respectively, which are consistent with metallic Pd.[40] In addition, two shoulders were also existed at binding energies of 341.8 and 336.7 eV related to oxidized Pd species. It also confirms the formation of Ag core Pd shell because only Pd shell exposes to the air during the sample preparation. Ag $3d_{5/2}$ and Ag $3d_{3/2}$ peaks are located at 367.6 and 374.1 eV, respectively which are in accordance with metallic Ag.[40]

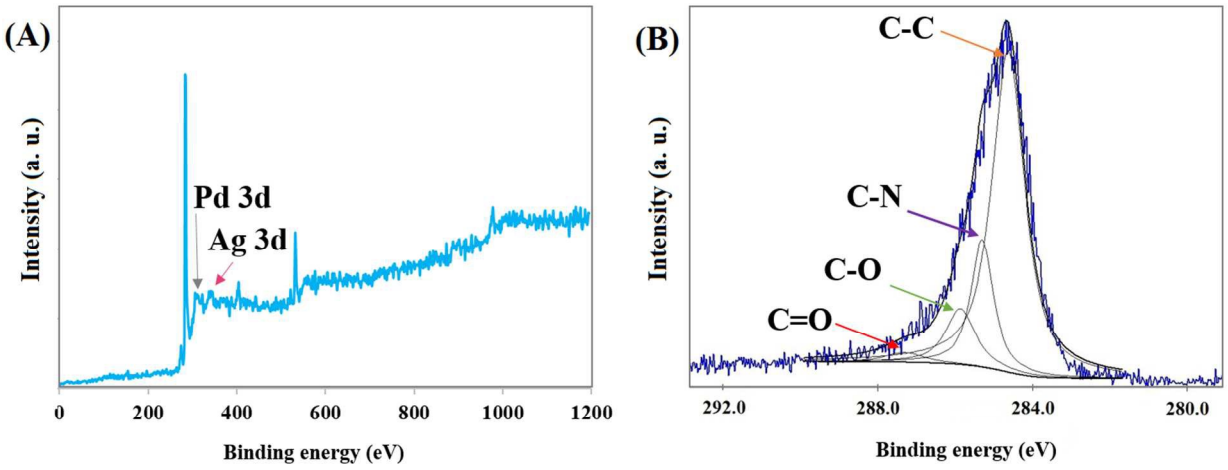

Fig. 4. XPS spectrum of Ag@Pd/N-GCNT aerogel (A), and high resolution XPS spectrum of C 1s (B).

3.2. Catalytic activity

The catalytic activity of the as synthesized Ag@Pd/N-GCNT aerogel was investigated for dehydrogenation of FA. We started our investigation by testing the different amounts of the catalyst. To this purpose, 0.002, 0.003, and 0.004 g Ag@Pd/N-GCNT aerogels were employed under the similar conditions. Increasing the amount of the catalyst from 2 mg to 3 mg results in decreasing the reaction time from 48 min to 35 min with approximately complete conversion but more increasing of the catalyst amount does not enhance the reaction significantly (Fig. 5). So, 3

View Article Online
DOI: 10.1039/C7NJ01108C

mg catalyst was chosen as the optimized catalyst amount at 25 ^{o}C for 1.5 mmol FA generating 66 mL gas in 35 min giving a TOF as high as 413 h^{-1} (See ESI for TOF calculations).

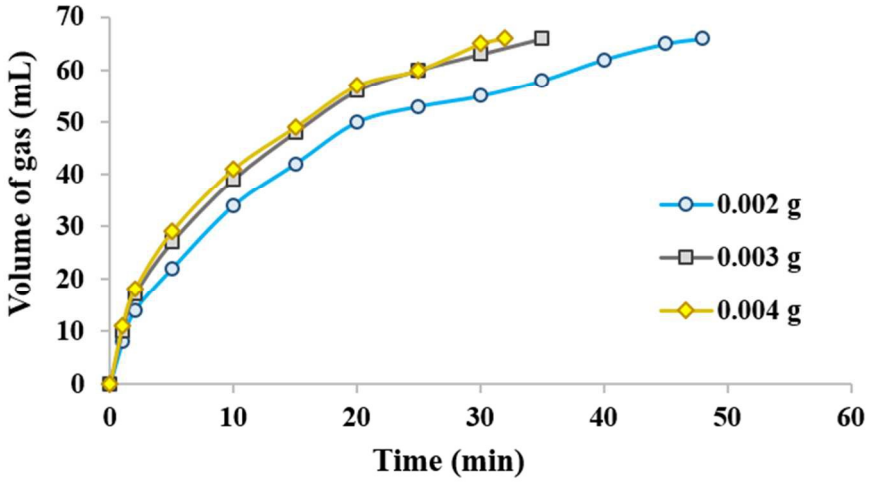

Fig. 5. The effect of catalyst amount on gas generation (25 ^{o}C and 3 mg catalyst).

The catalytic activity of Ag@Pd nanoparticles without support were examined to evaluate the effect of the support on the catalyst efficiency (Fig. 6). The reaction proceed until releasing 35 mL gas in 20 min indicating the decreased catalytic efficiency compared to Ag@Pd on the N-GCNT aerogel as the support. Actually, nitrogen doping promoted the electrical conductivity and metal immobilization by strengthening the metal-support interactions. In addition, the structure of graphene carbon nanotube aerogel can afford additional anchoring points for the metal nanoparticles. So, N-GCNT aerogel as the support enhance the catalytic activity for FA decomposition probably due to immobilization of the nanoparticles and inhibit them from aggregation. In addition, weakly basic amino groups may facilitate the cleavage of OH bond of FA which is related to the rate-determining cleavage of C-H bond from the $HCOO^{-}$ intermediate to release H_2.[41, 42]

View Article Online
DOI: 10.1039/C7NJ01108C

The catalytic activity of Ag/N-GCNT aerogel and Pd/N-GCNT aerogel were tested for dehydrogenation of FA. According to the results, Ag@Pd showed much better activity compared to singe metals counterparts because of the synergistic effect of two metals. As mentioned before, adding Ag to Pd enhance the catalytic performance because of electronic promotion effect and the charge transfer from Ag to Pd. The Ag/Pd ratio was also optimized to obtain the best metal composition in the catalyst. The composition of Ag/Pd in Ag@Pd/N-GCNT aerogel was modified by changing the designed molar ratio of $AgNO_3$ and $PdCl_2$, and measured using AAS, as shown in Table 1. Fig. 6 shows the gas generation from the FA system in the presence of $Ag_1@Pd_2$/N-GCNT, $Ag_1@Pd_1$/N-GCNT, and $Ag_2@Pd_1$/N-GCNT aerogels which the best result was attributed to $Ag_1@Pd_1$.

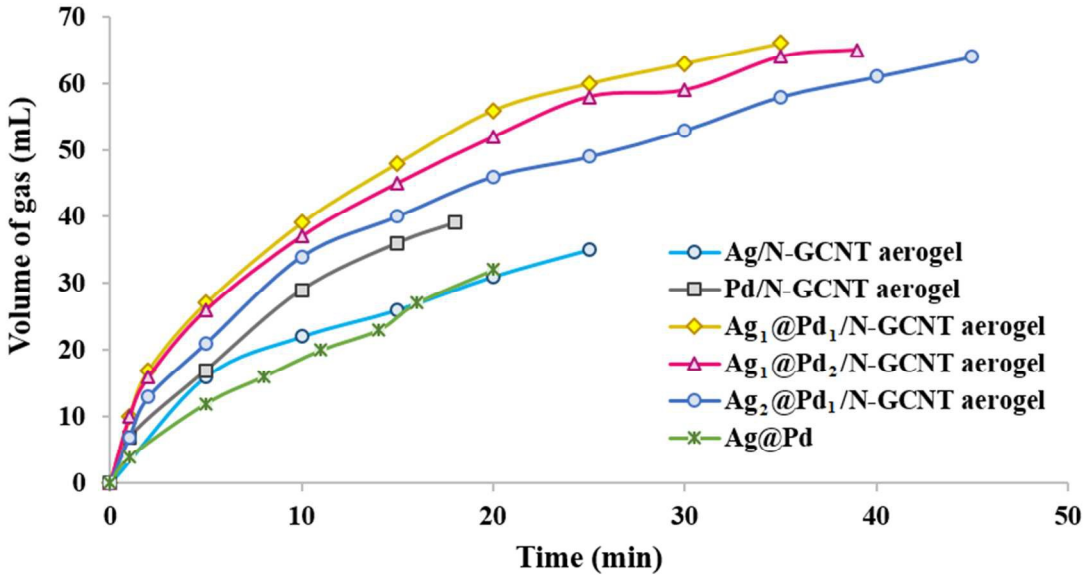

Fig. 6. Volume of the generated gas versus time for the dehydrogenation of FA over the different catalysts at 25 ^{o}C.

The catalytic dehydrogenation of FA was also carried out at different temperatures to obtain the activation energy (E_a) of this reaction (Fig. 7). Increasing the reaction temperature form 25 to 45

View Article Online
DOI: 10.1039/C7NJ01108C

and 60 °C enhance TOF of the reaction from 413 h^{-1} to 803 and 1446 h^{-1}, respectively. According to the Arrhenius plot of ln TOF vs. 1/T for this catalyst (Fig. 7), E_a was calculated to be 29.28 kJ mol^{-1} which is lower than most of the previously report for FA dehydrogenation (Table 2).

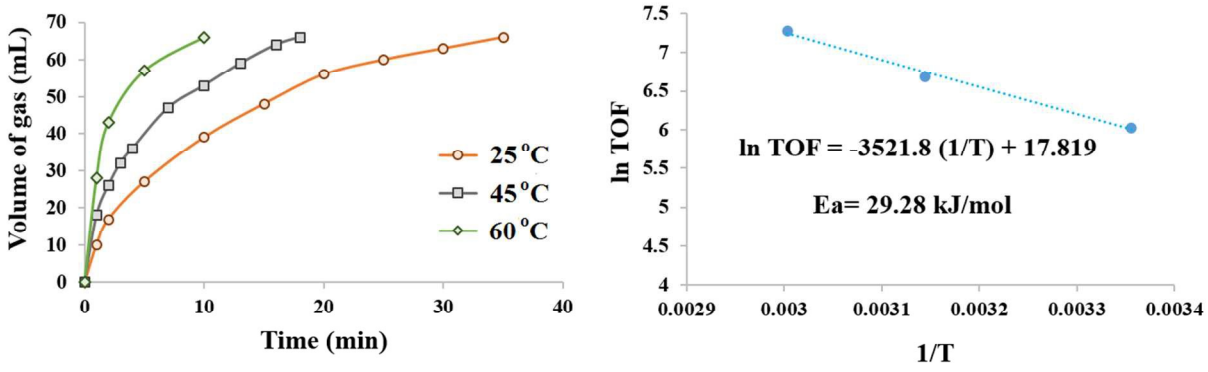

Fig. 7. Volume of the generated gas (CO_2 + H_2) versus time, Arrhenius plot (ln(TOF) vs. 1/T).

Another pathway for FA decomposition is a dehydration reaction releasing CO. To investigate the composition of generated gas, a trap containing 10 M NaOH solution was used to complete absorption of CO_2 from the as formed gas of the catalytic reaction.[43, 44] The volume of gas reduced to half the original value suggesting a volume ratio of CO_2 and H_2 to be 1:1. Moreover, the amount of CO was measured by GC spectrum which demonstrated no CO from the evolved gas. These results exhibited the generation of only CO_2 and H_2 without releasing CO. Therefore, the Ag@Pd/N-GCNT aerogel catalyst exhibited excellent H_2 selectivity for the decomposition of FA.

The heterogeneous nature of Ag@Pd/N-GCNT aerogel was investigated by removing the catalyst from the reaction mixture at half FA conversion. Further processing of the filtrate under the similar conditions did not increase the conversion. AAS analysis of the filtrate showed that the content of Ag and Pd in the solution were below the detection limit. These results confirmed the heterogeneous nature of Ag@Pd/N-GCNT aerogel.

View Article Online
DOI: 10.1039/C7NJ01108C

Table 2. Comparison of catalytic activities of AgPd-based catalysts for dehydrogenation of formic acid.

Catalyst	Solvent/medium	Temp. (^{o}C)	TOF (h^{-1})	Activation energy (kJ/mol)	Ref.
Ag@Pd/N-GCNT aerogel	**Aqueous**	**25**	**413**[a] 1183[b], 854.4[c], 613.3[d]	**29.28**	**Present work**
C-$Ag_{42}Pd_{58}$	Aqueous	50	365[c]	22	[24]
AgAuPd/rGO	Aqueous	25	73.6[d]	-	[45]
AgPd-Hs/G	Aqueous HCOONa	25	333[c]	28	[46]
$(Co_6)Ag_{0.1}Pd_{0.9}$/rGO	Aqueous HCOONa	50 25	2739[a] 453[a]	43.1	[47]
$Ag_{20}Pd_{80}$@MIL-101	Aqueous HCOONa	80	848[b]	27	[48]
AgPd@ZIF-8	Aqueous HCOONa	80	580[b]	51.38	[49]
Agglomerated Ag-Pd	Aqueous HCOONa	25	31.5[a]	-	[35]
$Ag_{0.1}$-$Pd_{0.9}$/rGO	Aqueous HCOONa	25	105.2[b]	-	[50]
AgPd/mCND/SBA-15	Aqueous HCOONa	50	893[b]	43.2	[51]

View Article Online
DOI: 10.1039/C7NJ01108C

$Ag_{74}Pd_{26}$/graphene	Aqueous HCOONa	25	572[d]	27.12	[43]
$Co_{1.6}Ag_{62.2}Pd_{36.2}$/graphene	Aqueous HCOONa	25	110[d]	33.9	[36]

[a] TOF were calculated after the reactions completions.
[b] Initial TOF were calculated during the first 5 min of the reactions.
[c] Initial TOF were calculated during the first 10 min of the reactions.
[d] Initial TOF were calculated during the first 20 min of the reactions.

The sustainable catalysts which decreases the cost and required time for replacing the spent catalyst with the fresh one are always highly desirable in chemical industries. The presence of N-GCNT aerogel provides the possibility for easy isolation of the catalyst form the reaction mixture which is very important for complete catalyst recovery. To investigate the catalyst recyclability, after the reaction completion, the catalyst was isolated by filtration or centrifugation, washed and dried to be used for the next run. The catalyst was employed for four runs without considerable loss in activity showing the stability of the presented catalyst (Fig. 8). It is worth mentioning that a little decrease in activity may be attributed to the increasing of the particle size.

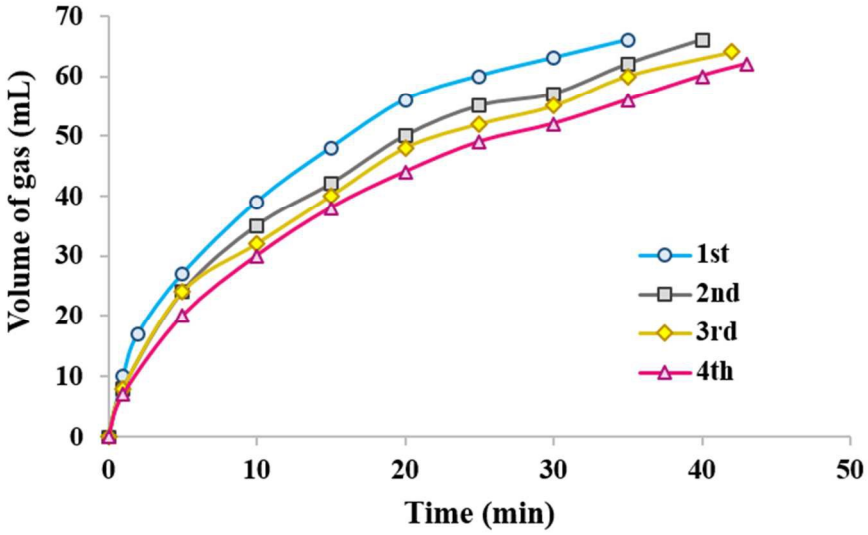

View Article Online
DOI: 10.1039/C7NJ01108C

Fig. 8. Stability test on the Ag@Pd/N-GCNT aerogel catalyst in the dehydrogenation of FA at 25 ^{o}C.

4. Conclusion

In this work, Ag@Pd nanoparticles immobilized on N-GCNT aerogel was synthesized and characterized by various analyses such as TEM, XPS, and BET. The high surface to volume ratio as well the nitrogen doping made N-GCNT aerogel suitable to stabilize metal nanoparticles. The low catalytic activity of support free Ag@Pd confirmed that N-GCNT aerogel was an excellent support because it causes the high dispersion and relatively small size of nanoparticles. Moreover, the enhanced catalytic activity for Ag@Pd/N-GCNT aerogel was observed compared to single metals counterparts suggesting the synergistic effect of two metals for FA dehydrogenation. The catalyst could be easily recycled by filtration or centrifugation and showing no significant loss in activity over four runs. The mild reaction conditions, no need to an additive, high activity, possibility of recycling, relatively low cost, and ease of applicability are some advantages of the Ag@Pd/N-GCNT aerogel catalyst for FA decomposition compared to most of the previously reports. These properties made the presented catalyst unique and suitable for practical and sustainable applications.

Acknowledgements

The financial support provided by the Iran National Science Foundation (INSF) is gratefully acknowledged.

References

1. A. Boddien, C. Federsel, P. Sponholz, D. Mellmann, R. Jackstell, H. Junge, G. Laurenczy and M. Beller, *Energy Environ. Sci.*, 2012, **5**, 8907-8911.
2. P. Moriarty and D. Honnery, *Int. J. Hydrogen Energy*, 2010, **35**, 12374-12380.
3. J. A. Turner, *Science*, 2004, **305**, 972-974.
4. S. Enthaler, *ChemSusChem*, 2008, **1**, 801-804.
5. M. Ojeda and E. Iglesia, *Angew. Chem. Int. Ed.*, 2009, **48**, 4800-4803.

View Article Online
DOI: 10.1039/C7NJ01108C

6. C. Fellay, P. J. Dyson and G. Laurenczy, *Angew. Chem. Int. Ed.*, 2008, **47**, 3966-3968.
7. M. Yurderi, A. Bulut, N. Caner, M. Celebi, M. Kaya and M. Zahmakiran, *Chem. Commun.*, 2015, **51**, 11417-11420.
8. P. Stathi, Y. Deligiannakis, G. Avgouropoulos and M. Louloudi, *Appl. Catal. A*, 2015, **498**, 176-184.
9. F. Bertini, I. Mellone, A. Ienco, M. Peruzzini and L. Gonsalvi, *ACS Catal.*, 2015, **5**, 1254-1265.
10. W. Gan, P. J. Dyson and G. Laurenczy, *ChemCatChem*, 2013, **5**, 3124-3130.
11. I. Schmidt, K. Müller and W. Arlt, Energy Fuels, 2014, **28**, 6540-6544.
12. M. Grasemann and G. Laurenczy, *Energy Environ. Sci.*, 2012, **5**, 8171-8181.
13. Z.-L. Wang, Y. Ping, J.-M. Yan, H.-L. Wang and Q. Jiang, *Int. J. Hydrogen Energy*, 2014, **39**, 4850-4856.
14. A. Bulut, M. Yurderi, Y. Karatas, M. Zahmakiran, H. Kivrak, M. Gulcan and M. Kaya, *Appl. Catal. B*, 2015, **164**, 324-333.
15. M. Martis, K. Mori, K. Fujiwara, W.-S. Ahn and H. Yamashita, *J. Phys. Chem. C*, 2013, **117**, 22805-22810.
16. M. Jeon, D. J. Han, K.-S. Lee, S. H. Choi, J. Han, S. W. Nam, S. C. Jang, H. S. Park and C. W. Yoon, *Int. J. Hydrogen Energy*, 2016, **41**, 15453-15461.
17. Y. Lykhach, M. Happel, V. Johánek, T. s. Skála, F. Kollhoff, N. Tsud, F. Dvořák, K. C. Prince, V. Matolín and J. r. Libuda, *J. Phys. Chem. C*, 2013, **117**, 12483-12494.
18. N. Yi, H. Saltsburg and M. Flytzani-Stephanopoulos, *ChemSusChem*, 2013, **6**, 816-819.
19. Q.-Y. Bi, X.-L. Du, Y.-M. Liu, Y. Cao, H.-Y. He and K.-N. Fan, *J. Am. Chem. Soc.*, 2012, **134**, 8926-8933.
20. Y. Mahendra, A. Tomoki, T. Nobuko and Q. Xu, *J. Mater. Chem.*, 2012, **22**, 12582-12586.
21. Z. L. Wang, J. M. Yan, Y. Ping, H. L. Wang, W. T. Zheng and Q. Jiang, *Angew. Chem. Int. Ed.*, 2013, **52**, 4406-4409.
22. J. M. Yan, Z. L. Wang, L. Gu, S. J. Li, H. L. Wang, W. T. Zheng and Q. Jiang, *Adv. Energy Mater.*, 2015, **5**, 1500107.
23. Z.-L. Wang, J.-M. Yan, H.-L. Wang, Y. Ping and Q. Jiang, *J. Mater. Chem. A*, 2013, **1**, 12721-12725.
24. S. Zhang, Ö. Metin, D. Su and S. Sun, *Angew. Chem. Int. Ed.*, 2013, **52**, 3681-3684.
25. C. Hu, X. Mu, J. Fan, H. Ma, X. Zhao, G. Chen, Z. Zhou and N. Zheng, *ChemNanoMat*, 2016, **2**, 28-32.
26. Q.-L. Zhu, N. Tsumori and Q. Xu, *Chem. Sci.*, 2014, **5**, 195-199.
27. Q. Y. Bi, J. D. Lin, Y. M. Liu, H. Y. He, F. Q. Huang and Y. Cao, *Angew. Chem. Int. Ed.*, 2016, **55**, 11849-11853.
28. B. F. Machado and P. Serp, *Catal. Sci. Tech.*, 2012, **2**, 54-75.
29. P. Serp, M. Corrias and P. Kalck, *Appl. Catal. A*, 2003, **253**, 337-358.
30. Q. Cheng, J. Tang, J. Ma, H. Zhang, N. Shinya and L.-C. Qin, *Phys. Chem. Chem. Phys.*, 2011, **13**, 17615-17624.
31. H. Wang, T. Maiyalagan and X. Wang, *ACS Catal.*, 2012, **2**, 781-794.
32. W. S. Hummers Jr and R. E. Offeman, *J. Am. Chem. Soc.*, 1958, **80**, 1339-1339.
33. J. H. Jung, D. S. Cheon, F. Liu, K. B. Lee and T. S. Seo, *Angew. Chem. Int. Ed.*, 2010, **49**, 5708-5711.
34. S. Kabiri, D. N. Tran, T. Altalhi and D. Losic, *Carbon*, 2014, **80**, 523-533.

View Article Online
DOI: 10.1039/C7NJ01108C

35. J. Liu, L. Lan, R. Li, X. Liu and C. Wu, *Int. J. Hydrogen Energy*, 2016, **41**, 951-958.
36. L. Yang, W. Luo and G. Cheng, *Int. J. Hydrogen Energy*, 2016, **41**, 439-446.
37. C.-T. Hsieh, Y.-Y. Liu, D.-Y. Tzou and W.-Y. Chen, *J. Phys. Chem. C*, 2012, **116**, 26735-26743.
38. D. Zhang, T. Yan, L. Shi, Z. Peng, X. Wen and J. Zhang, *J. Mater. Chem.*, 2012, **22**, 14696-14704.
39. G.-L. Tian, M.-Q. Zhao, Q. Zhang, J.-Q. Huang and F. Wei, *Carbon*, 2012, **50**, 5323-5330.
40. J. Chastain, R. C. King and J. Moulder, *Handbook of X-ray photoelectron spectroscopy: a reference book of standard spectra for identification and interpretation of XPS data*, Physical Electronics Division, Perkin-Elmer Corporation Eden Prairie, Minnesota, 1992.
41. K. Mori, M. Dojo and H. Yamashita, *ACS Catal.*, 2013, **3**, 1114-1119.
42. Z.-L. Wang, J.-M. Yan, Y.-F. Zhang, Y. Ping, H.-L. Wang and Q. Jiang, *Nanoscale*, 2014, **6**, 3073-3077.
43. L. Yang, X. Hua, J. Su, W. Luo, S. Chen and G. Cheng, *Appl. Catal. B*, 2015, **168**, 423-428.
44. K. Mandal, D. Bhattacharjee and S. Dasgupta, *Int. J. Hydrogen Energy*, 2015, **40**, 4786-4793.
45. S.-j. Li, Y. Ping, J.-M. Yan, H.-L. Wang, M. Wu and Q. Jiang, *J. Mater. Chem. A*, 2015, **3**, 14535-14538.
46. Y. Jiang, X. Fan, X. Xiao, T. Qin, L. Zhang, F. Jiang, M. Li, S. Li, H. Ge and L. Chen, *J. Mater. Chem. A*, 2016, **4**, 657-666.
47. Y. Chen, Q.-L. Zhu, N. Tsumori and Q. Xu, *J. Am. Chem. Soc.*, 2015, **137**, 106-109.
48. H. Dai, N. Cao, L. Yang, J. Su, W. Luo and G. Cheng, *J. Mater. Chem. A*, 2014, **2**, 11060-11064.
49. H. Dai, B. Xia, L. Wen, C. Du, J. Su, W. Luo and G. Cheng, *Appl. Catal. B*, 2015, **165**, 57-62.
50. Y. Ping, J.-M. Yan, Z.-L. Wang, H.-L. Wang and Q. Jiang, *J. Mater. Chem. A*, 2013, **1**, 12188-12191.
51. L. Xu, B. Jin, J. Zhang, D.-g. Cheng, F. Chen, Y. An, P. Cui and C. Wan, *RSC Adv.*, 2016, **6**, 46908-46914.

View Article Online
DOI: 10.1039/C7NJ01108C

Catalytic dehydrogenation of formic acid by silver palladium supported on nitrogen doped graphene carbon nanotube aerogel